Investigation of Kp- and Kd-atom formation and their collisional processes with hydrogen and deuterium targets by the classical-trajectory Monte Carlo method

M. Raeisi G.[1,2] and S. Z. Kalantari[1,*]

[1]*Department of Physics, Isfahan University of Technology, Isfahan 84156-83111, Iran*

[2]*Department of Physics, Shahrekord University, Shahrekord 115, Iran*

(Received 19 July 2010; published 4 October 2010)

The classical-trajectory Monte Carlo method has been used to study the capture of negative kaons by hydrogen and deuterium atoms; subsequently, the elastic scattering, Stark mixing, and Coulomb deexcitation cross sections of Kp and Kd atoms have been determined. The results for kaonic atom formation confirm the initial conditions that have been parametrically applied by most atomic cascade models. Our results show that Coulomb deexcitation in Kp and Kd atoms with $\Delta n > 1$ is important in addition to $n = 1$. We have shown that the contribution of molecular structure effects to the cross sections of the collisional processes is larger than the isotopic effects of the targets. We have also compared our results with the semiclassical approaches.

DOI: 10.1103/PhysRevA.82.042501 PACS number(s): 36.10.Gv, 34.10.+x, 34.90.+q

I. INTRODUCTION

A kaonic atom, Kx ($x = p,d$), is formed when a beam of negative kaons enters a target of hydrogen or deuterium. The kaon loses its kinetic energy through the ionization and excitation of atoms and molecules of the target and is eventually captured, replacing the electron, in an excited state. Such atoms are called exotic atoms. They are usually formed in highly excited states; then, they are deexcited by competitive cascade processes [1]. The x-ray transitions to the lowest orbits are affected by the presence of the strong interaction between the nucleus and kaon. The measurements of the x-ray transitions, provide fundamental information on the low-energy kaon-nucleon interactions. Quantities such as kaon-nucleon scattering lengths can be determined by comparing the Deser-Truman formula with the measured shift and width of the K_α x-ray [1,2].

The kaonic hydrogen measured by the DEAR Collaboration (on DAΦNE) with an unprecedented precision, led to a lively debate on the kaon-proton scattering length extraction procedure [2]. The SIDDHARTA experiment started in early 2009, with more precise measurement for Kp atoms, which would be prepared for the kaonic-deuterium x-ray measurement [3].

The atomic cascade can reveal important information about the properties of kaonic atoms such as x-ray yield, cascade time, kinetic-energy distribution, and reaction with atoms in excited states [4,5]. The atomic cascade models are essential to understand the details of atomic transitions in various experimental conditions such as density [4–6].

The distributions of n,l states and kinetic energy at the instant of kaonic-atom formation are needed to calculate the cascade dynamics. In most previous calculations, some approximated distributions have been used [4]. Because in the case of muonic and antiprotonic atoms, classical-trajectory Monte Carlo calculations (CTMC) of collisional processes were in fair agreement with the semiclassical approaches [7] at the intermediate states, we use this method for kaonic atoms. Particularly, this method is more efficient than either full quantum mechanics or semiclassical approaches in highly excited states, where the Bohr correspondence principle is better satisfied.

The aim of this paper is to determine the cross sections of kaon capture by hydrogen and deuterium atoms, excitation and impact-ionization (processes 1), and collisional transitions such as Coulomb transition, Stark mixing, and elastic scattering of kaonic atoms (processes 2) by the CTMC method.

$$\begin{aligned} K + X_{1s} &\rightarrow (Kx)_{nl} + e, \\ K + X_{nl}, & \\ K + x + e. & \end{aligned} \tag{1}$$

$$\begin{aligned} (Kx)_{n_i l_i} + X, X_2 &\rightarrow (Kx)_{n_f l_f} + X, \\ (Kx)_{n_f l_f} + X_2, & \\ (Kx)_{n_f l_f} + X_2^*(X + X), & \end{aligned} \tag{2}$$

where $x = p,d$ and $X = \mathrm{H,D}$.

We are interested in the role of the Coulomb acceleration in highly excited states and in the competition between the accelerating process and slowing down in quasielastic collisions. Both molecular and atomic targets are used in our calculation in order to investigate the role of molecular and isotopic effects. In each case we compare our results with semiclassical approaches.

The paper is organized as follows. The CTMC method is described in Sec. II, the results of the calculations of kaon capture and collisional transitions for Kp and Kd atoms are presented in Sec. III. Finally, the conclusions are summarized in Sec. IV.

II. CTMC CALCULATION

At the beginning of the atomic cascade, where high nlm states are involved in the collisions, classical mechanics is expected to be a good approximation. By CTMC method, we can simulate the collisions of exotic atoms with the atoms or molecules of a target in the framework of classical trajectories. To learn more details about this method, the pioneering work of Percival and Arbines [8] and its applications in muon capture [9] and stripping reactions [10] are recommended.

In this model, to study the scattering of kaonic atoms in atomic or molecular targets, we consider the kaonic atoms

*Corresponding author: zafar@cc.iut.ac.ir

and targets as classical particles. In the collisional transitions, the electrons are assumed to be fixed charge distributions corresponding to the $1s$ atomic state. The following degrees of freedom are included in the model (Fig. 1): (Q_1, Q_2, Q_3) are coordinates of kaon relative to nucleus x in the Kx atom, (Q_4, Q_5, Q_6) are coordinates of the center of mass of the Kx atom relative to the center of mass of the X_2 molecule, and (Q_7, Q_8, Q_9) are coordinates of the nucleus X relative to the other nucleus X in the X_2 molecule.

A. Effective potential

The kaonic atoms are described as a classical two-body system with potential

$$V_{kx} = -\frac{1}{r_{Kx}}, \tag{3}$$

where r_{Kx} is the distance between the kaon and nucleus x.

The kaonic atom interacts with an atom of the target whose electron distribution is assumed to be frozen in the ground atomic state with the potential [7]

$$V_{Kx\text{-}X} = \left(\frac{1}{R_{KX}} + 1\right) e^{-2R_{KX}} - \left(\frac{1}{R_{xX}} + 1\right) e^{-2R_{xX}}, \tag{4}$$

where R_{KX} is the distance between the kaon and one nucleus X of the X_2 molecule, and R_{xX} is the distance between nucleus x in the Kx atom and one nucleus X of the X_2 molecule. The interaction between the atoms in the molecule is described by the Morse potential [11]

$$V_M(R_{XX}) = D_e\left(e^{-\alpha(R_{XX}-R_0)} - 1\right)^2, \tag{5}$$

where R_{XX} is the distance X in the molecule X_2, $D_e = 4.75$ (4.74) eV, $\alpha = 1.03$ (1.04), and $R_0 = 1.41a_0$ ($1.42a_0$) for H_2 (D_2) [11]. The total effective potential is the summation of the three parts.

B. Method of calculation

For the four-body system shown in Fig. 1, we have used the generalized coordinates Q_i and momenta P_i where $i = 1,2,\ldots,9$. To obtain the classical equations of motion, we should calculate the potentials (3)–(5) as a function of the generalized coordinates Q_i. For this purpose, distances r_{Kx}, R_{KX}, R_{xX}, and R_{XX} should be derived from the generalized coordinates Q_i by a set of appropriate canonical transformations from Cartesian coordinates of the kaon, x, and X particles in Fig. 1, to the generalized coordinates Q_i [10].

After eliminating the center-of-mass coordinates of the entire system, the 18 coupled differential equations for generalized coordinates and momenta can be obtained by Hamilton's equations. These equations of motion with the total effective potential are solved using a fourth-order Runge-Kutta method with variable step size. The quasiclassical initial conditions are defined as follows. By considering the initial principal quantum number n_i and the orbital angular momentum l_i of Kx atom, the initial classical states are generated as a classical Kepler orbit with the bound energy E_{ni} and the classical angular momentum l_c:

$$E_{n_i} = -\frac{\mu_K}{2n_i^2}, \quad l_c = l_i + \frac{1}{2}, \tag{6}$$

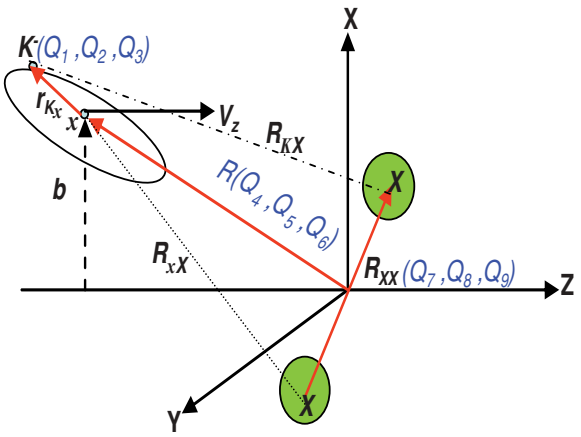

FIG. 1. (Color online) Classical four-body system with the generalized coordinates $Q_i, i = 1,\ldots,9$. b is an impact parameter, and V_z is the initial relative velocity of the Kx atom and X_2 molecule.

where μ_K is the reduced mass of Kx atom. The orbit is oriented randomly in space, and the orbital Kx motion is set at a random time within the period. The atoms in the target molecule are set by distance R_{XX}, which is randomly selected by one of the turning points, R_+ or R_-. They are determined as follows:

$$V_M(R_{XX}) = E_{0,0}, \tag{7}$$

where $E_{0,0}$ is the rotational-vibrational ground-state energy of molecule. Consequently, Eq. (5) is easily solved by Newton's method. The values ($R_- = 1.2a_0$, $R_+ = 1.7a_0$) and ($R_- = 1.22a_0$, $R_+ = 1.61a_0$) have been obtained for H_2 and D_2, respectively. The molecule is randomly oriented in space. The impact parameter b of the Kx atom is selected with a uniform distribution in the interval $(0, b_{\max})$. For a given initial state n of the Kx atom and laboratory kinetic energy E_i, a set of impact parameters b_i are generated, where $i = 1,\ldots,N$, and N is the total number of the classical trajectory of the kaonic atom. The optimum value for $b_{\max}$ is found to be equal to $5 + 2n_i/\mu_K$. The conservation of total energy, linear momentum, and angular momentum is checked in the numerical procedure. Instead of requiring convergence for every individual trajectory, we have used the global criteria in which the cross sections for various processes were stable in the statistical errors.

The final atomic state is determined when the distance between the center of mass of the Kx atom and target molecule after collision, R in Fig. 1, is larger than $10\,a_0$. The final atomic state $n_f l_f$ with the energy E_{Kx} and the angular momentum l_c is identified by the following rules [12]:

$$n - \frac{1}{2} < n_c \leqslant n + \frac{1}{2}, \quad l_f < l_c \frac{n_f}{n_c} \leqslant l_f + 1. \tag{8}$$

The adjustment factor n_f/n_c ensures that the inequality $l_f < n_f$ will be satisfied. In addition to the quantum numbers n_f and l_f, the scattering angle θ at the laboratory and the excitation energy of the molecular target, ΔE_{target}, are also obtained. The cross sections are obtained from the computed set of trajectories using the following procedure. If p_i^c is considered as the probability of the reaction (2) in channel c,

which corresponds to either Coulomb transition, Stark mixing, or elastic scattering in ith collision, i.e.,

$$p_i^c = \begin{cases} 1, & \text{if channel } c \text{ occurred} \\ 0, & \text{otherwise} \end{cases} \tag{9}$$

then the cross section for the reaction in channel c is given by

$$\sigma_c = 2\pi b_{\max} \frac{1}{N} \sum_{i=1}^{N} b_i p_i^c. \tag{10}$$

It should be noted that the same procedure is used for calculating the cross sections of kaon interactions with atoms or molecules of the target in reaction (1).

III. RESULTS

Because the number of the calculated cross sections is very large, only a small part of the results, such as l-averaged cross sections, are shown here.

A. Kaon capture

To obtain reliable initial conditions for cascade calculations, the cross sections of the processes 1 and 2 are determined in the energy region 0.01 eV–10 keV. Our calculations show that the contribution of capturing and elastic scattering is higher than inelastic channels (ionization + excitation). Figure 2 shows that the capturing cross section approaches zero by increasing energy. Elastic scattering cross sections tend to value close to the classical limit. Also due to the similarity in electronic structure of hydrogen and deuterium targets, the isotopic effect is negligible. Values of inelastic scattering cross sections (ionization and excitation) are increased at the above ionization potential, while they are smaller than elastic scattering cross sections.

On the basis of the capturing cross section, the n_i and l_i distributions are obtained for kaon kinetic energy $E_0 = 1.0$ eV.

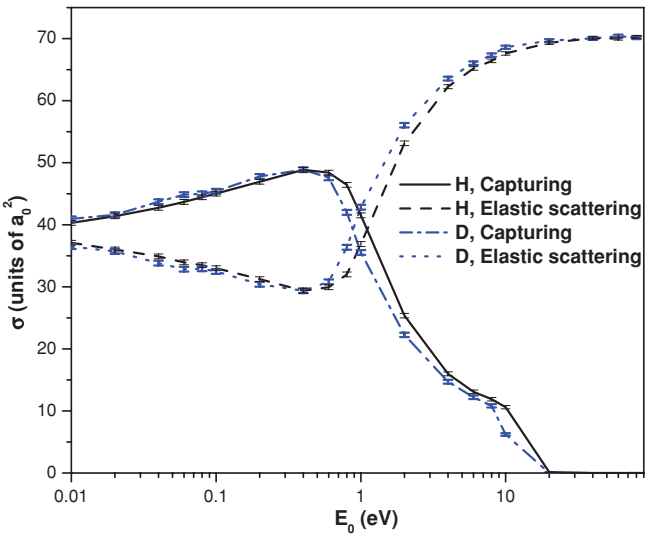

FIG. 2. (Color online) Capturing and elastic-scattering cross sections of kaon in H and D targets for different initial kinetic energies of kaon (E_0).

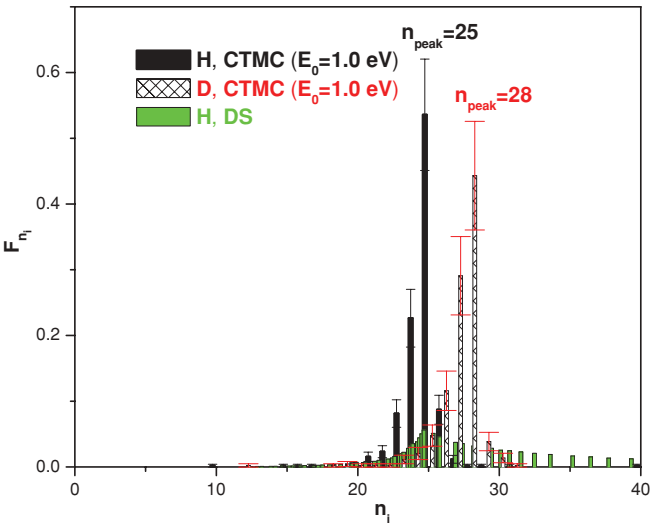

FIG. 3. (Color online) The n_i distribution of the capture of kaon in H and D targets. The results of the quantum DS approach for H have also been shown [13].

Also, they can be compared with the results of quantum diabatic-state approach (DS) [13] in Figs. 3 and 4. The values in agreement with the DS approach at least at the peak of the n distribution for the Kp case. Another comparison can be made with the values corresponding to a statistical distribution, which is used for most atomic cascade models. Furthermore, the peaks of the n_i distributions confirm the classical crude estimation, $\sqrt{\mu_K/m_e}$, which are 25 and 27 for Kp and Kd atoms, respectively. Finally, in this energy region, n, l and the kinetic-energy distributions of the formed kaonic atoms are independent of kinetic energy of kaon. Figure 5 shows the kinetic-energy distributions of the formed Kp and Kd atoms. It is shown that the average kinetic energy of kaonic atoms is not very sensitive to the initial kinetic energy of kaons.

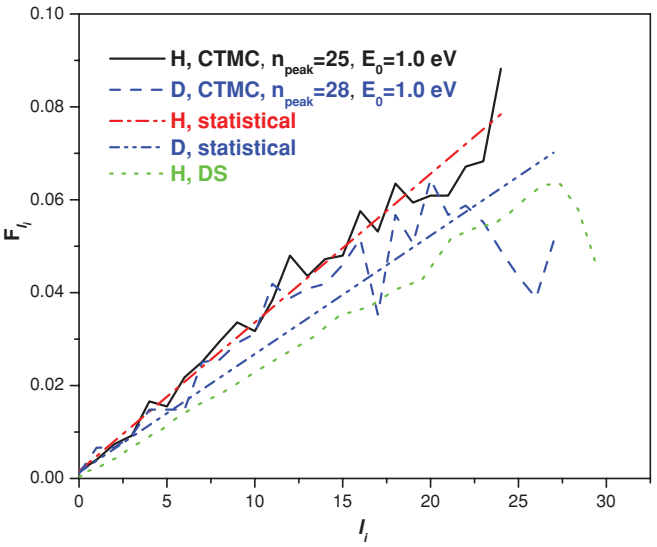

FIG. 4. (Color online) The l_i distribution of the capture of kaon in H and D targets. The results of quantum DS approach for H have also been shown [13].

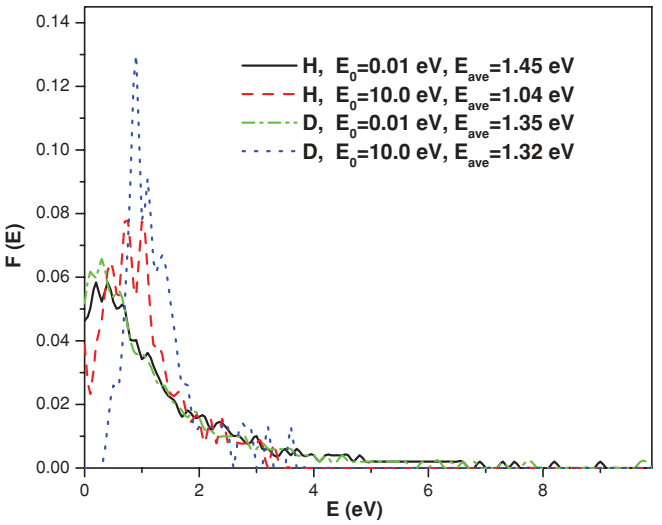

FIG. 5. (Color online) The kinetic-energy distribution of the formed Kp and Kd atoms for different initial kinetic energies of kaon (E_0). The mean values of the kinetic energy of kaonic atoms are also indicated.

B. Collisional processes

1. Stark mixing and elastic scattering

A neutral Kx atom penetrates into the target, where the electric field mixes the sublevels with the same n and different l (linear Stark effect). Stark mixing affects the population of the nl sublevels. It is particularly important since it results in strong absorption during the cascade by feeding the ns states [4]. The first detailed calculation of the Stark-mixing cross section was done semiclassically by Leon and Bethe [14]; then, it was extended by Terada and Hayano [15]. In this article we have calculated Stark-mixing cross sections of Kp atoms by the CTMC method. In Fig. 6, the n dependence of the CTMC Stark-mixing cross sections is shown in comparison with semiclassical results at $E_i = 1.0$ eV. It shows that the

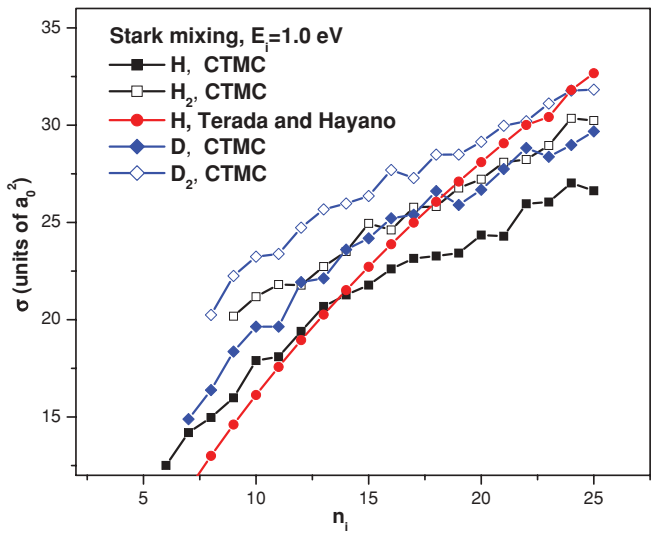

FIG. 6. (Color online) The n-dependence of Stark-mixing cross sections for atomic and molecular targets at $E_i = 1.0$ eV. The semiclassical results for Kp atoms are also shown by filled circles.

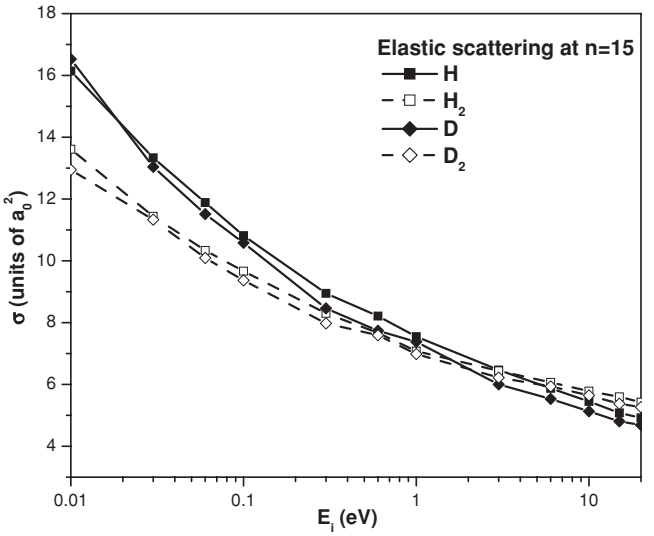

FIG. 7. The energy dependence of elastic-scattering cross sections for atomic and molecular targets at $n = 15$.

molecular effects are important for all of the levels, because the electric field due to the two proton or deuteron nuclei in the molecule is greater than that in atoms. Our calculations show that for low states, our results are good in agreement with semiclassical results. But at large n they are different, because the large n belongs to the classical limit in which the semiclassical results are not precise. Therefore, the results of CTMC for Stark-mixing cross sections can be used for cascade calculations in any n states.

The elastic scattering leads to the deceleration of kaonic atoms if the kinetic energy is larger than the average kinetic energy of the target atoms. This mechanism, together with the Stark transition, influences the kinetic-energy distribution of Kp atoms during the cascade transitions. The CTMC results for the energy dependence of the elastic-scattering cross sections, averaged on l states for $n = 15$, are shown in Fig. 7. It shows that the elastic-scattering cross section has a decreasing behavior with respect to energy. The isotopic effects are negligible, while the atomic and molecular structures are important especially at low energies. As expected, at high energies, the cross sections tend to their classical limits.

2. Coulomb deexcitation

The mechanism of this process is similar to Stark mixing. If a stronger electric field is applied on the neutral Kx atom by atomic or molecular targets during the collision, it can mix states with different values of n. In this process, the transition energy of the exotic atom is shared between the colliding particles. It is an important accelerating mechanism that produces high kinetic energy of kaonic atoms. It has been shown experimentally for muonic [16] and pionic hydrogen [17]. Therefore, it may broaden the widths of the x-ray spectrum at low states due to a Doppler broadening effect [5]. At first, a Coulomb transition of the Kp atom and dissociation of the hydrogen molecule in the center of mass of the entire system have been simulated by CTMC method. The results are shown in Fig. 8. It can be seen that the Kp atom with an initial

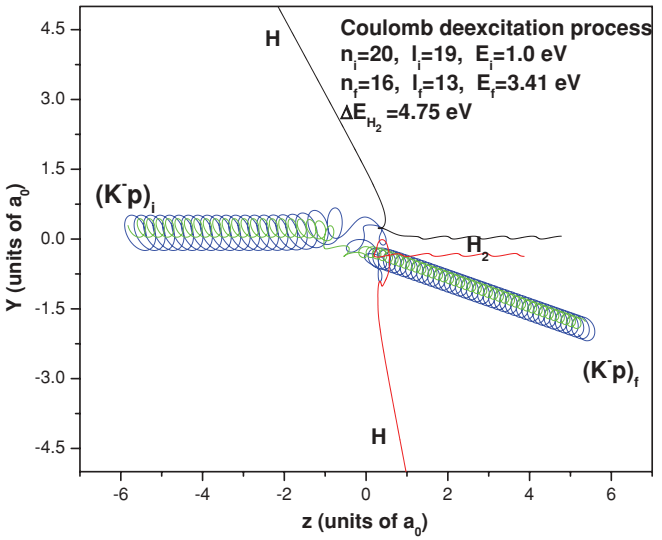

FIG. 8. (Color online) An example of a $(Kp)_i + H_2 \rightarrow (Kp)_f + H + H$ collision with impact parameter $b = 0.5a_0$ resulting in Coulomb deexcitation.

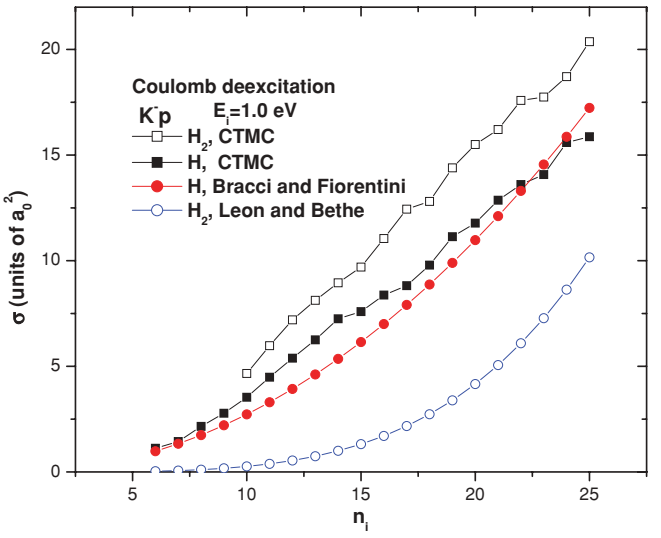

FIG. 10. (Color online) The comparison of the n-dependence of Coulomb deexcitation cross sections for different approaches in laboratory kinetic energy $E_i = 1.0$ eV.

state of $n_i = 20, l_i = 19$, and $E_i = 1.0$ eV moves from the left, and the hydrogen molecule moves from the right. In the final state, the Kp atom has $n_f = 16, l_i = 13$, and $E_f = 3.41$ eV.

In Fig. 9, the n_f dependence of the Coulomb deexcitation cross sections has been shown for kaonic hydrogen with $n_i = 15$ and 25 and $E_i = 1.0$ eV. This shows that the distribution of the cross sections versus the final state n_f is completely different for the molecular and atomic targets for high-n_i states, particularly at high-n_f states. Figure 9 also shows that the transitions with $\Delta n > 1$, which are ignored for μp and πp atoms, are important for Kx atoms.

The n_i dependence of the total cross sections of the Coulomb deexcitation at $E_i = 1.0$ eV is compared with other works in Fig. 10. Initially, Leon and Bethe estimated phenomenologically the cross section of this process for the H_2 molecule with its so-called chemical dissociation [14], which was used in many cascade calculations. Their estimation was in order of the size of the exotic atoms ($\pi a_n^2/2$, where a_n is the nth Bohr radius of the exotic atom). It is not a good estimation, as Fig. 10 shows that CTMC results for collision with H_2 are greater than the Leon and Bethe estimation. Therefore, we expect that the chemical dissociation has a greater contribution to cascade dynamics in high excited states. Then, Bracci and Fiorentini applied a semiclassical approach to the collision of muonic hydrogen with a H atom [18]. They showed that this approach is better justified by increasing the mass of the exotic particle. As expected, it is in fair agreement with the CTMC results for kaonic atoms.

The isotopic effect, as indicated in Figs. 11 and 12, is not large, since the cross sections are not very different from each other. Figures 10 and 11 show that the Coulomb cross sections increase by increasing n_i. Our calculations show that

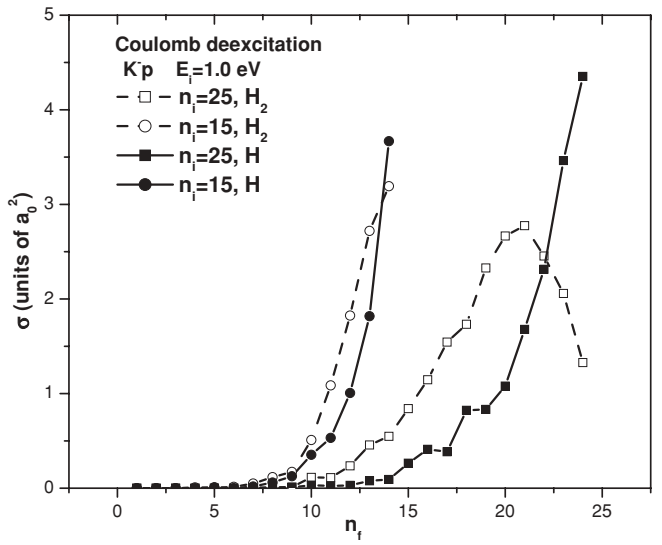

FIG. 9. The n_f dependence of Coulomb deexcitation cross section in H and H_2 targets with $n_i = 15, 25$ and the laboratory kinetic energy of Kp atoms being $E_i = 1.0$ eV.

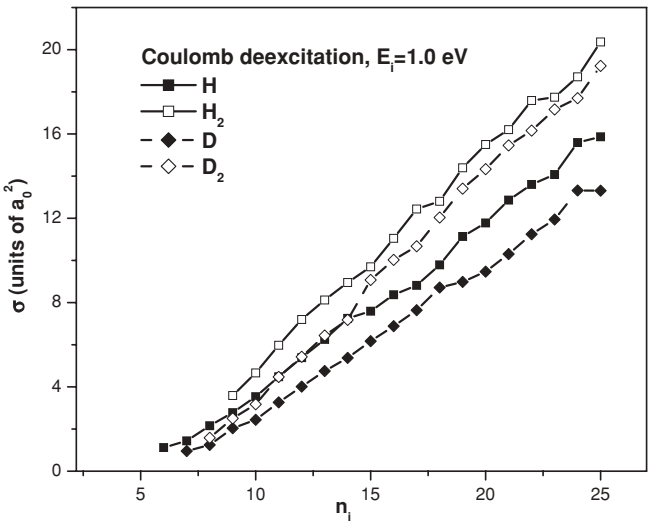

FIG. 11. The n_i-dependence of Coulomb deexcitation cross sections for atomic and molecular targets at $E_i = 1.0$ eV.

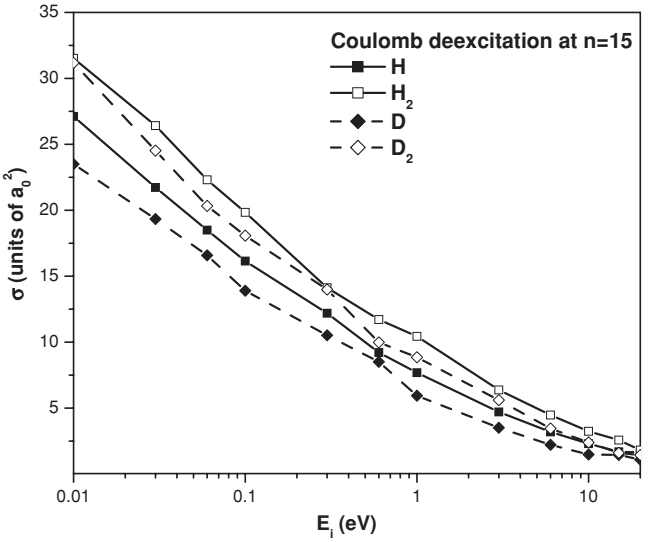

FIG. 12. The energy dependence of Coulomb deexcitation cross sections for atomic and molecular targets at $n = 15$.

the Coulomb cross sections have a decreasing behavior with collision energy (Fig. 12). Semiclassical calculations have predicted a $\frac{1}{\sqrt{E}}$ behavior of the cross sections [18] which can be confirmed by CTMC calculation in high energies (Fig. 12), because in high energy the values of the cross sections from semiclassical calculations get close to classical calculated values.

IV. CONCLUSIONS

The CTMC method was applied to study kaon capture on H and D atoms and the collisional processes of the kaonic atoms with atomic and molecular targets which are important for atomic cascade calculations. In general, the following results were obtained.

(I) Kaon capture: The cross section of kaon capture is important around the ionization energy of the target. In this energy region n_i, l_i, and the kinetic-energy distribution of the formed kaonic atoms are independent of kaon kinetic energy. The calculations show that the most probable of the principal quantum numbers n are 25 and 28 for Kp and Kd atoms, respectively, which are in agreement with the quantum DS approach and classical crude estimation. The l distributions are also close to traditional statistical values. These results confirm some initial conditions that have been used in most atomic cascade models with some tuning parameters. However, more precise calculations using our n distribution for the formed Kp and Kd atoms are suggested.

(II) Collisional processes: Stark mixing that leads to mixing sublevels for different l is effectively important at high-n states and intermediate kinetic energies of kaonic atoms. The cross sections of Kd atoms are more than those of Kp atoms. This is due to the smaller size of the Kd atom compared with the Kp atom. The Stark mixing in Kx atoms by molecules is more important than that by atoms, because the electric field is produced more by the molecule on the penetrated Kx atom. Our results agree with semiclassical results; however, they are different at large n_i. Since the large n_i is the classical limit, the CTMC results are more precise at large n_i. Thus, our results can be used in any n_i states.

The Coulomb deexcitation process is important at high-n states and low collisional energies that agree fairly well with the semiclassical results. We have shown that the Coulomb transitions with $\Delta n > 1$ are also important for Kx atoms. The transitions with $\Delta n > 1$ may result in atoms with higher kinetic energy. Also the molecular structure effects are dominant compared with isotopic effects.

The cross sections of elastic scattering have a smooth decreasing behavior versus the kinetic energy of Kx atoms. The isotopic effects are negligible, while the molecular structure is important for elastic scattering cross section at low energies.

The CTMC method can be improved by including the electron degrees of freedom in the calculations, which will allow us to calculate cross sections for ionization of the target. It is the same as the Auger transition in quantum mechanics. For this purpose we should use an updated version of the CTMC-Fermion molecular dynamic (FMD) method [19], which offers a constrained potential preventing the system from occupying quantum mechanically forbidden regions of phase space.

[1] D. Gotta, Prog. Part. Nucl. Phys. **52**, 133 (2004).
[2] G. Beer *et al.*, Phys. Rev. Lett. **94**, 212302 (2005).
[3] C. Curceanu Petrascu *et al.*, Eur. Phys. J. A **31**, 537 (2007); J. Marton *et al.*, in *Proceedings of the International Conference on Muon Catalyzed Fusion and Related Topics (μCF-07), 18–21 June 2007, Dubna, Russia*, edited by L. I. Ponomarev *et al.* (Joint Institute for Nuclear Research, Dubna, 2007), p. 214.
[4] M. Raeisi G. and S. Z. Kalantari, Phys. Rev. A **79**, 012510 (2009).
[5] S. Z. Kalantari and M. Raeisi G., Phys. Rev. C **81**, 014608 (2010).
[6] T. S. Jensen and V. E. Markushin, Eur. Phys. J. D **19**, 165 (2002); Lect. Notes Phys. **627**, 37 (2003).
[7] T. S. Jensen and V. E. Markushin, Eur. Phys. J. D **21**, 271 (2002).
[8] R. Arbines and I. C. Percival, Proc. Phys. Soc. **88**, 861 (1966); **88**, 873 (1966).
[9] J. S. Cohen, Phys. Rev. A **27**, 167 (1983).
[10] M. Karplus, R. N. Porter, and R. D. Sharma, J. Chem. Phys. **43**, 3259 (1965); R. E. Olson and A. Salop, Phys. Rev. A **16**, 531 (1977).
[11] B. H. Bransden and C. J. Joachain, *Physics of Atoms and Molecules* (Longman Scientific and Technical, Essex, 1983).
[12] R. E. Olson, Phys. Rev. A **24**, 1726 (1981).
[13] J. S. Cohen, R. L. Martin, and W. R. Wadt, Phys. Rev. A **24**, 33 (1981).
[14] M. Leon and H. A. Bethe, Phys. Rev. **127**, 636 (1962).
[15] T. P. Terada and R. S. Hayano, Phys. Rev. C **55**, 73 (1997).
[16] R. Pohl, Diss. ETH No.14096, Zurich, 2001 (unpublished).
[17] J. Schottmuller *et al.*, Hyperfine Interact. **119**, 95 (1999); A. Baderstcher *et al.*, Europhys. Lett. **54**, 313 (2001).
[18] L. Bracci and G. Fiorentini, Novo Cimento **213**, 9 (1977).
[19] J. S. Cohen, Phys. Rev. A **56**, 3583 (1997).